ISBN: 978-3-95450-247-9 ISSN: 2673-5490 doi: 10.18429/JACoW-IPAC2024-WEPS61

# MAPPING THE STRAY MAGNETIC FIELD AT THE RELATIVISTIC HEAVY ION COLLIDER TUNNEL*

P. Xu†, Q. Wu, H. Witte, A. Drees, G. Mahler, Y. Bai
Brookhaven National Laboratory, Upton, United States



*Abstract*

A new Rapid Cycling Synchrotron (RCS) [1] is designed to accelerate the electron bunches from 400 MeV up to 18 GeV for the Electron Ion Collider (EIC) [2] being built at Brookhaven National Laboratory (BNL). One of the two Relativistic Heavy Ion Collider (RHIC) rings will serve as the Hadron Storage Ring (HSR) of the EIC. Beam physics simulations for the RCS demonstrate that the electron beam is sensitive to the outside magnetic field in the tunnel. Significant magnetic fields are expected due to the HSR and the Electron Storage Ring (ESR) being at full energy during the RCS operation. The earth magnetic field at the location of the RCS center was measured throughout the circumference of 3,870 m tunnel without RHIC operation. In addition, the fringe magnetic fields from RHIC magnets at several locations during RHIC operation were measured. A robotic technology is being developed to automatically measure the stray magnetic field at any location during the RHIC (or future EIC) operation.

## INTRODUCTION

The EIC will collide high energy and highly polarized hadron and electron beams with luminosities up to $10^{34}$ $cm^{-2}s^{-1}$ [3]. The RCS was designed to accelerate the electron beams from 400 MeV up to 18 GeV to enter the ESR for the EIC. The electron beams are sensitive to the outside magnetic field due to the 400 MeV low injection energy. At some locations of the ring, the ESR is located right on top of the RCS, the supporting materials (e.g., cast iron) needed for the ESR will also affect the magnetic field around the RCS. Mapping the stay magnetic field at the RCS location is important for its design. A schematic of the different rings in the EIC is shown in Fig. 1 [2].

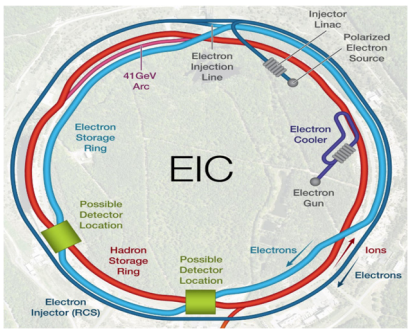


Figure 1: Overhead schematic of EIC.

* Work supported by Brookhaven Science Associates, LLC under Contract No. DE-SC0012704 with the U.S. Department of Energy.
† email address: pxu@bnl.gov.

## EXPERIMENTAL METHOD

### *AlphaLab MR3 Sensor*

The 3-axis magneto resistive milligauss meter (MR3) from the AlphaLab [4] was used as one option to measure the stray magnetic field due to its high resolution (0.01 mG) and high accuracy (±0.5%). However, they can measure only up to 2 G. The MR3 sensor (shown in Fig. 2) is mounted on a tripod so that its height can be adjusted, shown in Fig. 3. The RCS locations (Fig. 1) are relatively consistent along the ring, where it is located about 40 cm from the tunnel wall and about 35 cm from the ground.


Figure 2: The MR3 sensor used to measure the magnetic field at the RCS location.

Figure 3: Experimental setup for the MR3 sensor.

### *Smart Phone Sensor*

There are typically magnetic sensors located in the latest smart phones, where the phyphox [5] app can be installed to measure the magnetic field. The advantages of the phone sensors are easy to use with high resolution (0.1 mG) and relatively high range (50 G). Since the phone sensor is wireless, it can be easily mounted on a rolling cart to measure the magnetic field while it is moving. A simple setup with the phone sensor is shown in Fig. 4.

### *Comparison between MR3 and phone sensors*

The measurement of the magnetic field for comparison between the sensors was performed at 6 locations, shown in Fig. 5. The comparison between the MR3 sensor and the phone sensor is shown in Fig. 6, with good agreement.

ISBN: 978-3-95450-247-9 ISSN: 2673-5490 doi: 10.18429/JACoW-IPAC2024-WEPS61

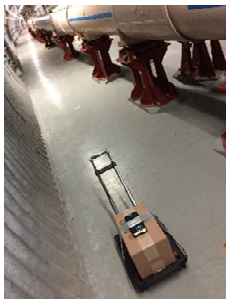

Figure 4: Experimental setup for the phone sensor.

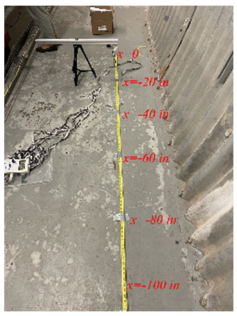

Figure 5: Measured locations for the comparison

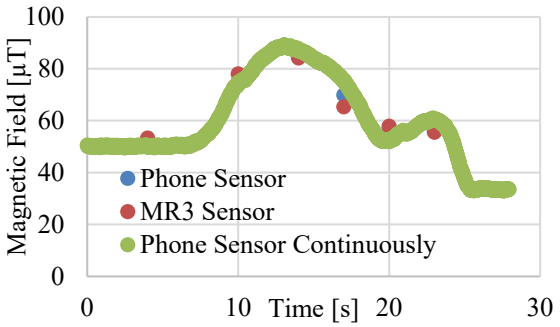


Figure 6: Comparison of the measured magnetic field between the MR3 and the phone sensor, the discrete points are the measured 6 locations, the continuously points are the data measured continuously with the phone sensor.

## RESULTS AND DISCUSSION

### *Stray magnetic field without RHIC operation*

The stray magnetic field without RHIC operation was measured along the RCS locations of the entire ring, with the circumference 3,870 m. An example of the sector 7 and its measured magnetic field are shown in Fig. 7 and Fig. 8, respectively.

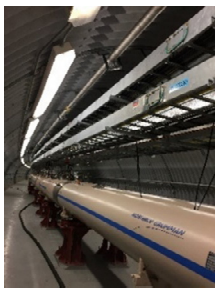

Figure 7: Sector 7 of the RHIC tunnel

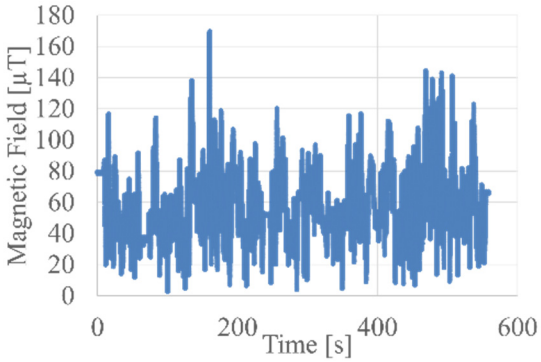


Figure 8: Measured stray magnetic field at RCS locations of sector 7, as an example.

The maximum and average stray magnetic field at the RCS locations of the entire RHIC tunnel is shown in Fig. 9. The average stray magnetic field is about 0.5 G, close to the earth magnetic field of Upton, New York in 2023. The maximum field is close to 2 G at each sector, but it is only at very few locations. The reason of field close to 2 G might be due to the rebar buried underground that affects the measurements. The locations of where the maximum field measured and the field directions is shown in Table 1, where the field direction X is along the tunnel, Y is across the tunnel, and Z is perpendicular to the ground.

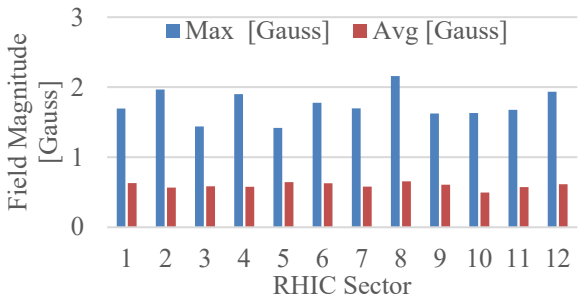


Figure 9: Measure maximum and average stray magnetic field at the RCS locations of different sectors without RHIC operation

Table 1: Locations and field direction of the maximum measured stray magnetic field

| Sector | Max Location | Field Direction |
|---|---|---|
| 1 | Q8DU7 | Z/X |
| 2 | Q10 | Z |
| 3 | D17Q17 | Z |
| 4 | D5, D19 | Z |
| 5 | D9 | Z |
| 6 | Q3 | Z |
| 7 | Q15 | Z |
| 8 | D6Q7 to Q7 | Z |
| 9 | D11 | Z/Y |
| 10 | Q9 | Z |
| 11 | D6 | Z |
| 12 | D15Q16 | Z |

ISBN: 978-3-95450-247-9 ISSN: 2673-5490 doi: 10.18429/JACoW-IPAC2024-WEPS61



### *Stray magnetic field with RHIC operation*

The experimental setup to measure the stray magnetic field during RHIC operation is shown in Fig. 10, where the sensor S1 is located close to the RCS location, sensor S2 and S3 are mounted on the tripods to measure the magnetic field at the same level as the magnet.


Figure 10: Experimental set up to measure the magnetic field during RHIC operation

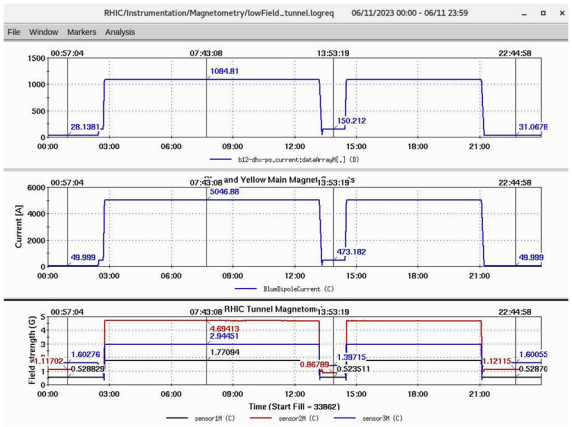


Figure 11: Stray magnetic field at close the DX magnet of sector 12 during RHIC operation, sensor 1M refers to the field magnitude at sensor S1.

The stray magnetic field distribution with current is shown in Fig. 11, where the current was ramping up and down and the measured field was changing with the current. Four currents and their measured stray field at the three sensors are shown in Table 2, where B1 refers to the field magnitude of the sensor S1. At low current (I<650 A), the measured field at sensor S1 is close to the earth magnetic field, the data at S2 and S3 also stayed at similar values. At full current (I=6131.7 A), the measured field at sensor S1 increased to 1.77 G, the data at sensor S2 and sensor S3 also increased.

Table 2: Measured field at different current

| **Total I** [A] | **B1** [G] | **B2** [G] | **B3** [G] |
|---|---|---|---|
| 78.1 | 0.53 | 1.12 | 1.6 |
| 81.1 | 0.53 | 1.12 | 1.6 |
| 623.4 | 0.52 | 0.87 | 1.4 |
| 6131.7 | 1.77 | 4.69 | 2.94 |

### *Automatically measure the field*

Two independent solutions have been developing to automatically measure the field at the RHIC tunnel. The first one is the "SPOT" [6] built by Boston Dynamics [7]. A test has been made at the RHIC tunnel (Fig. 12). First, map the route using the remote controller and save the route; second, run the SPOT automatically following the saved map and record the locations while measuring the magnetic field. The locations of the magnetic sensor and the measured field are synchronized using the time in the magnetic sensor and the SPOT.

Another solution is using the line following function from a robot car, shown in Fig. 13, which has also been tested in the tunnel. The robot car has a camera that can read the color of the line, thus it follows the line.

Figure 12: The SPOT at the RHIC tunnel.

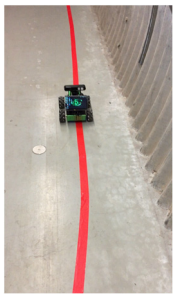

Figure 13: Line following robot car at the RHIC tunnel.

## CONCLUSION

The stray magnetic field at the RCS locations of the RHIC tunnel has been mapped out through the whole tunnel without operation. The measured average field is close to the earth magnetic field, the maximum field is close to 2 G. The stray magnetic field at the RCS locations during RHIC operation has also been measured at several locations (12-DX, 12-Triplet, Alcove 11c arc, and 9-Q2). The maximum measured field at the RCS location is 1.77 G at 12-DX during operation. Two robot systems have been developed to map the field at the whole tunnel during RHIC operation automatically. The next step is to measure the magnetic field automatically using the developed magnetic field.

## ACKNOWLEDGEMENTS

The authors would like to thank Warren Stern, Yonggang Cui, and Odera Dim from the Non-proliferation and national Security department of BNL for useful discussions.

ISBN: 978-3-95450-247-9 ISSN: 2673-5490 doi: 10.18429/JACoW-IPAC2024-WEPS61

# REFERENCES


[1] V. H. Ranjbar, F. Meot, H. Lovelace III, and F. Lin, "EIC's Rapid Cycling Synchrotron Spin Tracking Update", in *Proc. 13th Int. Particle Acc. Conf. (IPAC2022)*, Bangkok, Thailand, June 2022, paper THP0ST004, pp. 2439-2441. doi: 10.18429/JACoW-IPAC2022-THPOST004

[2] F. Willeke and J. Beebe-Wang, "Electron Ion Collider Conceptual Design Report 2021 (No. BNL-221006-2021-FORE; TRN: US2215154)", OSTI.GOV, 2021. doi:10.2172/1765663

[3] H. Witte *et al.*, "The interaction region of the electron-ion collider EIC", in *Proc. 13th Int. Particle Acc. Conf. (IPAC2021)*, Campinas, SP, Brazil, May 2021. paper WEPAB002, pp. 2574-2577. doi: 10.18429/JACoW-IPAC2021-WEPAB002

[4] https://www.alphalabinc.com/products/mr3

[5] S. Staacks, S. Hütz, H. Heinke, and C. Stampfer, "Advanced tools for smartphone-based experiments: phyphox", *Physics Education*, vol. 53, no. 4, p.045009, May 2018. doi:10.1088/1361-6552/aac05e

[6] W. Stern, "Autonomous and Semi-Autonomous Robots Working Group Forming at the Lab", Brookhaven National Laboratory Monday Memo, Feb. 2021.

[7] E. M. Wetzel, J. Liu, T. Leathem, and A. Sattineni, "The use of boston dynamics SPOT in support of LiDAR scanning on active construction sites", *Proceedings of the International Symposium on Automation and Robotics in Construction (ISARC2022),* vol. 39, pp. 86-92. doi:10.22260/ISARC2022/0014